36th International Electric Vehicle Symposium and Exhibition (EVS36)
Sacramento, California, USA, June 11-14, 2023

Effects of Bi-directional Charging on the Battery Energy Capacity and Range of a 2018 Model Year Battery Electric Vehicle

Aaron Loiselle-Lapointe[1], Yeong Yoo[2], Samuel Pedroso[3], Aaron Conde[3]

[1] *(corresponding author) Environment and Climate Change Canada, 335 River Road, Ottawa, K1A0H3, Canada, Aaron.Loiselle@ec.gc.ca*

[2] *National Research Council Canada, 1200 Montreal Road, Ottawa, K1A0R6, Canada*

[3] *Transport Canada, 330 Sparks Street, Ottawa, K1A0N5, Canada*

Executive Summary

Two identical 2018 battery electric vehicles (BEVs) were mileage accumulated to approximately 18,000 km. One of the BEVs was additionally subjected to V2G activities, including bidirectional charging (BDC), intermittently during mileage accumulation. Environment and Climate Change Canada conducted chassis dynamometer testing programs to determine the baseline range, energy consumption rates and energy battery energy capacities of the two BEVs at 1,600 km, and then again at the conclusion of the study at 18,000 km. The two BEVs performed nearly identically at the beginning of the study (baseline). After 18,000 km mileage accumulation, 3 years and 220 BDC cycles totalling 3.66 MWh of discharge energy on one of the BEVs, the two BEVs both lost approximately 8% of their useable battery energy. SOC management during BDC activities and the high storage SOC of the Control BEV are likely the primarily reasons for the similar battery degradation rates of two BEVs.

Keywords:V2G, vehicle performance, BEV, battery SOC, battery ageing

1 Introduction

Battery electric vehicles (BEVs) are still an emerging market technology in the transportation sector when compared to long established internal combustion engine vehicle technologies. While much research has been, and continues to be, conducted on the effects of various operational conditions on BEV performance, vehicle battery and infrastructure technologies are evolving at such a rate that knowledge gaps continue to appear. Two such gaps include battery capacity degradation and the effects of bi-directional charging (BDC) on a BEV's performance and durability; distinguished journals have devoted entire publication issues to the subject of lithium-ion battery aging [1]. Continuous charging and discharging of a battery, whether it be due to on-road driving or BDC, can have the same final effect: loss of battery capacity due to physical and chemical degradation of the battery cells [2]. Researchers in the field of battery degradation have noted that BDC can potentially degrade a BEV's battery more quickly [1, 3 and 4] than if the BEV was simply charged after being driven.

In any emerging market technology, information about the product's performance under reasonable usage conditions is a requirement for establishing consumer buy-in and trust, and to allow consumers to make informed decisions [3]. Further, as BDC becomes more prominent, it will present a growing issue for vehicle manufacturers and regulators because warranties and durability standards/regulations are currently based on the vehicle's calendar age and mileage, neither of which capture BDC activities. For this issue, a conversion factor from BDC usage hours to vehicle mileage would be ideal, but also very different to establish via an objective and universally acceptable method.

Numerous modelling studies have been conducted to piece together a comprehensive characterization of the effects of BDC on lithium battery technologies [5-12]. There is no simple answer to the question: how does BDC impact battery degradation. This is because there is a plethora of strategies with which to perform BDC, and thus numerous impacts of those strategies on battery degradation. What has been asserted by the research community, however, is that real world data is vital to establish the robustness and accuracy of simulations and models that estimate battery degradation due to vehicle-to-grid (V2G) activities, including BDC [3, 4 and 13]. However, as noted by [4], most of the studies in available literature are based on simulations, and do not include empirical data from real world battery testing, save for a handful of studies [14 and 15].

Environment and Climate Change Canada (ECCC), the National Research Council (NRC) and Transport Canada (TC) have collaborated to investigate the impact of BDC on a BEV's battery degradation. This paper presents the comparative results of this chassis dynamometer test program applied for two identical model year 2018 BEVs; one with mileage accumulation only and the other with both mileage accumulation and V2G operation.

2 Method

Two TC owned 2018 model year BEVs (one Control BEV and one BDC BEV) were mileage accumulated to 1,600 km, after which they underwent baseline chassis dynamometer testing in environmental chambers at the Emission Research and Measurement Section (ERMS) of ECCC. Following this, TC accumulated between 135-180 km/day on the Control BEV and the BDC BEV concurrently. During accumulation, drivers were instructed to set the cabin settings to 22°C year-round and higher if needed during the winter seasons. Throughout the mileage accumulation of both vehicles, the NRC periodically paused the on-road accumulation to conduct V2G testing on the BDC BEV. The NRC performed these V2G tests by subjecting the BDC BEV to a daily duty cycle comprised of frequency regulation (FR) for 2 hours and peak shaving (PS) for 4 hours, using the V2G testing facility located at the Canadian Centre for Housing Technology (CCHT) [16]. Specifically, a 2-hour average standard deviation signal as a part of the frequency regulation duty-cycle signal in a Sandia National Lab's report [17] was chosen and used for testing the secondary frequency control (SFC) and a 4 hour PS with C/5-rate for discharging and charging steps was used for testing the PS in a daily duty-cycle. In total, the NRC conducted 220 bi-directional cycles equalling a total of 3.88 MWh charging and 3.66 MWh discharging on the BDC BEV. To provide context, if the test vehicles were driven on-road using this 3.66 MWh, they would accumulate approximately 16,000 km (using an average energy consumption rate from both test vehicles over all drive cycles and temperatures tested in this study). After the NRC concluded their V2G program, the vehicles were periodically exercised on road during the COVID-19 pandemic, until the ERMS took possession of the vehicles and conducted a second round of chassis dynamometer tests in 2021. The timeline for this entire study, along with the monthly environmental conditions (pertinent to mileage accumulation and exercising portions of this study) are shown in Figure 1. As can be observed from Figure 1 the vehicles were subjected to average temperatures ranging from -17ºC to 30ºC [18].

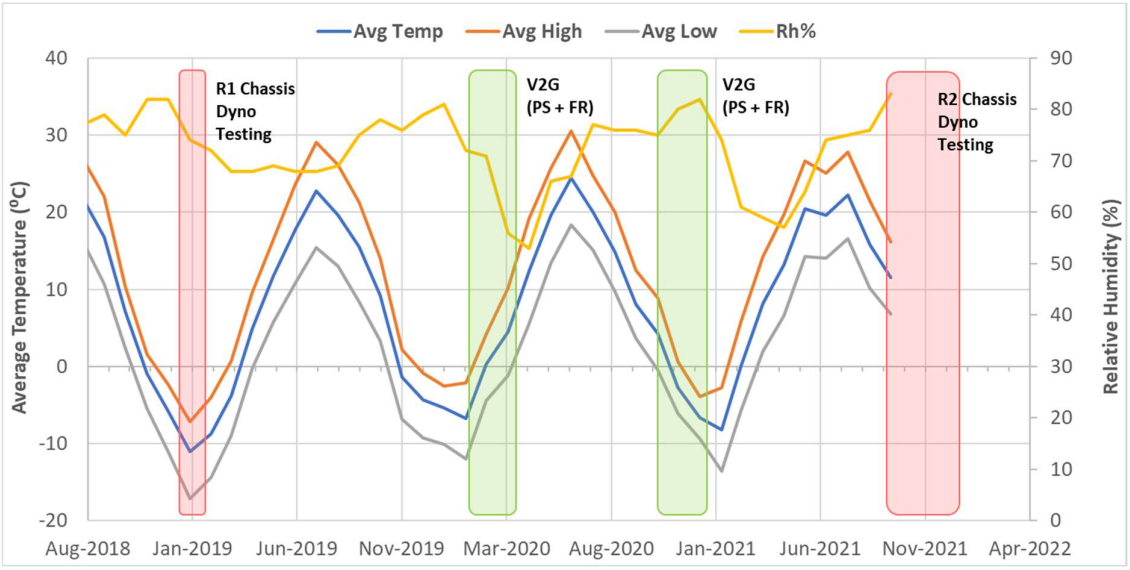

Figure 1: Study timeline and environmental conditions [18]

2.1 Test Setup

At ECCC's Emissions Research and Measurement Section (ERMS), the test vehicles underwent a series of full-depletion tests (FDTs) on a chassis dynamometer. The test vehicles were driven over the SAE J1634 Multi-Cycle Test (MCT), the SAE J1634 SC03 FDT, and a NYCC FDT, at temperatures of -7°C, 25°C and 35°C [19]. During the -7°C and 35°C tests, cabin temperature was set to 22°C with automatic fan control. The test matrix for each vehicle is provided in Table 1. Interruptions and delays to the test program due to the global COVID-19 pandemic resulted in some test conditions not being evaluated.

Table 1: Test sequence repeats for each vehicle, temperature and testing round

Round	Odometer [km]	Test Specimen	-7°C		25°C		35°C	
			US06 MCT	NYCC FDT	US06 MCT	NYCC FDT	NYCC FDT	SC03 FDT
1	1,607	Control BEV			3			
	1,603	BDC BEV			2			
2	18,845	Control BEV	2	2	2		2	2
	17,725	BDC BEV	2	1	2	2		2

2.2 Chassis Dynamometer

A Burke-Porter 4-wheel chassis dynamometer system with 122cm diameter roll was used to subject the two test vehicles to realistic loading at a range of speeds. Published road load 'target' coefficients describing the resistive force polynomial as a function of vehicle speed for this model of BEV were used to determine the chassis dynamometer 'set' coefficients at 25ºC according to the SAE J1263 procedure [20]. The same target road load coefficients were increased by 10% when used to determine the chassis dynamometer 'set' coefficients at an ambient temperature of -7ºC.

Dynamometer files were logged for each in-lab test, which captured the chassis dynamometer's loading and roller speed and, combined with the coastdown curve and equivalent vehicle test weight (ETW), were used to calculate various other parameters, including, but not limited to distance travelled, propulsion force, brake force, total propulsion energy and total brake energy.

2.3 Test Sequences

As described in section 2.1, both BEVs were subjected to a variety of transient and steady speed driving while on the ERMS chassis dynamometers. The specific test sequences are illustrated in Figure 2. Note that the middle and end constant speed cycles (CSC) are used to deplete the battery pack to keep total test time to a minimum, and the CSC times depend on the vehicle's range, and the energy intensiveness of the transient cycles in the test sequence. In Figure 2 the CSC and soak durations were adjusted to result in identical test times for each test sequence for easier visualization. In every test, the cycles were driven by a technician to the standards outlined in the U.S. Code of Federal Regulations Title 40 Part 86.115-78 (40CFR§86.115-78) [21]. As per the SAE J1634 recommended practice, a full-depletion test sequence concluded when the technician could no longer maintain the trace within the speed margins defined in 40CFR§86.115-78.

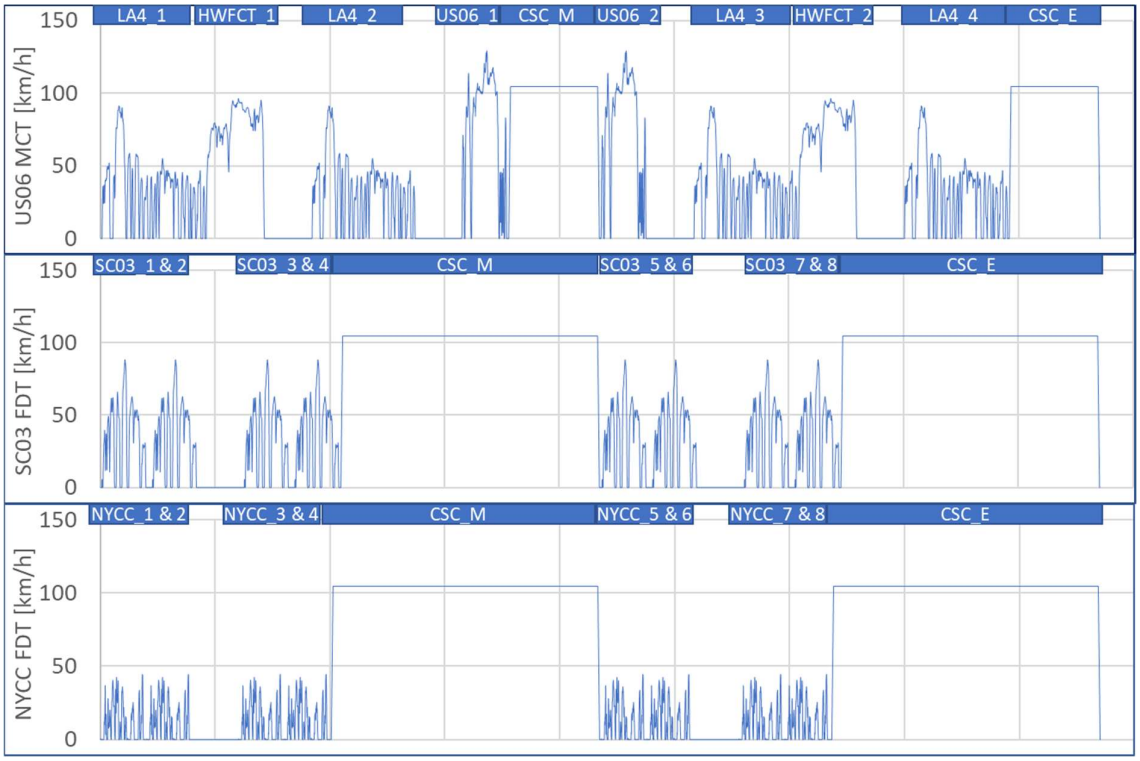

Figure 2: US06 MCT, SC03 FDT and NYCC FDT test sequence speed traces

2.4 Test Equipment

During in-lab testing a HIOKI PW6001-16 power analyser was used in conjunction with CT6843 current probes and voltage leads to accurately measure the electrical energy of the components shown in Figure 3. The HIOKI PW6001-16 samples at 5 Mhz, calculates instantaneous power and integrates the measurements to calculate cumulative current, and cumulative energy.

For the mileage accumulation portion of this study, Transport Canada used FleetCarma (now GeoTab) CANbus data loggers to record the real-time second-by-second vehicle metrics shown in Table 2. The CANbus data logger was also used during V2G activities to log this same data. In addition to the CANlogger data collected in Table 2, and of primary importance to the V2G activities, a supervisory control, and data acquisition (SCADA) system controlled and monitored the vehicle-to-grid interaction activities. The particulars for this aspect of the study are described in detail in [16].

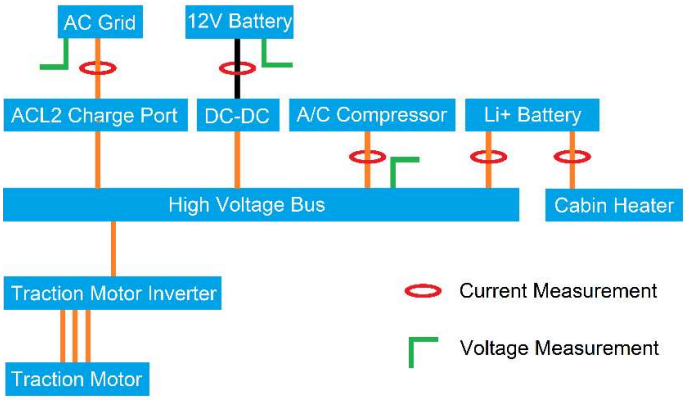

Figure 3: Current and voltage measurement locations along the BEV powertrain

Table 2: CANbus measurements made during On-Road Accumulation and V2G Activities

Electrical	HVAC	Environmental
Battery SOC	Battery Temperature	Date and Time
Battery Voltage	Outside Ambient Temperature	Odometer
Battery Current	AC Power	Speed
Max and Min Cell Voltages	Heater Power	GPS

2.5 Test Vehicles

Two identical model 2018 V2G capable BEVs with published ranges of 240 km, 40kWh batteries and utilizing front wheel drive powertrains were used for this study. The test vehicles are equipped with PTC cabin heaters, battery heating elements and passive battery cooling systems. Both vehicles were purchased new and underwent the first round of chassis dynamometer testing after 1600 km of break-in accumulation.

2.6 Calculations

The HIOKI power analyser files were used to calculate DC energy consumption (EC_{DC}) (for each test), useable battery energy (UBE) from each full test day, and full-recharge energy (FRE) and the full-recharge energy received by the battery (FRE_{DC}) from each full recharge of the battery pack. These calculations were made according to the equations and procedures in the SAE J1634 recommended practice [19]. Similarly, the chassis dynamometer measurements described in Section 2.2 were used to calculate the all-electric range and estimate the theoretical wheel loading and braking energy.

The battery pack C-rates were calculated for each measurement interval of each chassis dynamometer and mileage accumulation test file in order to allow for the creation of histograms representing the percentage of time each BEV spent in discrete ranges of C-rates. This resulted in more than 1700 individual histograms: one for each chassis dynamometer test file and mileage accumulation file.

3 Results and Discussion

3.1 Temperature and Drive Cycle

At the start of this study, after both vehicles were mileage accumulated to the break-in distance of 1600 km, they were tested at the ERMS using the SAE J1634 US06 Multi-Cycle Test (MCT) at 25ºC. The resulting FRE's, FRE_{DC}'s and UBE's differed between the Control and BDC BEVs by only 1%. Similarly, the calculated ranges for the LA4, HWFCT, CSC, and US06 drive cycles differed between the two vehicles by between 0% and 1%.

In the second round of testing, the vehicles had accumulated approximately 18,000 km (see Table 1) and the test schedule was expanded to evaluate the BEVs' performances at 35ºC, -7ºC and 25ºC. Figure 4 presents

the calculated ranges for each of the tested drive cycles at -7ºC, 25ºC and 35ºC and for both BEVs based on the round 2 measured energy consumptions and UBEs. The error bars represent one standard deviation from the average value, and for the instances where entire bars are missing those test conditions could not be evaluated (see Section 2.1). The NYCC and US06 drive cycles resulted in the lowest ranges at all test temperatures. This is unsurprising given that the NYCC covers only 2 km in 10 minutes, and the US06 is a highly aggressive drive trace. The Control BEV's 25ºC LA4 range exhibits an exceptionally large spread. This was due to one of the test repeats collecting less than 50% of the regenerative braking energy captured in the other repeat. The chassis dynamometer files were analysed for differences in loading and speed fluctuations, but none could be found. Chassis dynamometers have a so-called 'augmented braking' feature that is meant to reduce the braking load required by a vehicle's friction brakes. This feature must be deactivated when testing electric vehicles, otherwise the vehicle will be deprived of potential regenerative braking energy. During this study, therefore, technicians were instructed to deactivate the augmented braking feature of the chassis dynamometer for all tests. All the physical documentation collected for each test indicates augmented braking was indeed deactivated for the tests, but the dynamometer files do not record any information related to augmented braking so this cannot be verified through the data, and thus remains a remotely possible explanation for the differences in regenerative braking energy recorded between these tests, and the tests described below.

From Figure 4 the reader can observe that the BDC BEV's ranges are generally shorter than those of the Control BEV. As will be discussed in Section 3.2 the Control and BDC BEVs' energy capacities degraded in a very similar pattern and magnitude. Thus, the differences in range should be attributed to the energy consumption rates. Indeed, when analysed, the Control BEV's ECdc rates are generally lower than those of the BDC BEV and when compared between Rounds 1 and 2 the BDC BEV's ECdc rates are observed to increase by between 9% and 13%. The chassis dynamometer propulsion loads were almost identical between the Control and BDC BEVs. Similarly, the electrical propulsion effort of the BEVs' motors were also near identical to one another. However, the Control BEV recovered more regenerative braking energy during testing than the BDC BEV during identical testing. While the dynamometer braking loads were slightly higher for the Control BEV than the BDC BEV, the regenerative braking energy captured by the Control BEV far exceeds this difference. The modest differences in regenerative braking energy between the Control BEV and BDC BEV (varying between no difference and 318 Wh) for individual cycles quickly extrapolated to a large impact in range when combined with the test day's UBE, as can be seen in Figure 4. Additionally, the difference in regenerative braking energies between the Control BEV and the BDC BEV increased vastly (5-fold) from Round 1 testing to Round 2 testing. The reason for this large discrepancy in performance could not be determined with the available data.

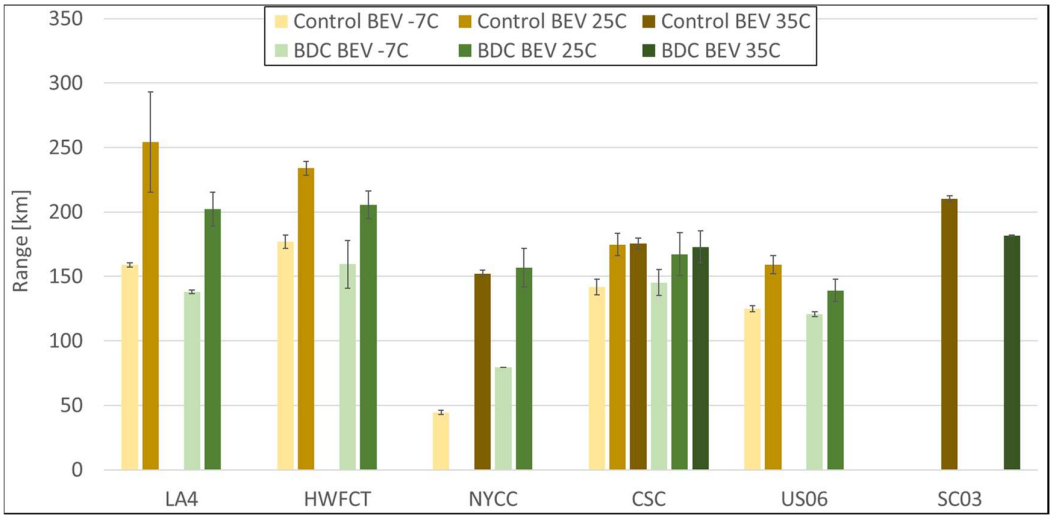

Figure 4: Round 2 Calculated Ranges for the Control and BDC BEVs for all tested conditions

3.2 Comparison Between V2G and Control BEV Energy Degradations

Figure 5 presents the 25ºC AC grid full recharge energy (FRE), the DC energy received by the battery from the FRE (FRE_{DC}) and useable battery energy available to the driver (UBE) for both vehicles during both rounds of testing. Between rounds 1 and 2 the FRE decreased by 10% for the Control BEV and 9% for the BDC. Similarly, the UBE decreased by 8% for both vehicles. As the first round of testing did not include -7ºC or 35ºC testing, the energy degradations between the test rounds for these temperatures was not determined. The authors previously conducted a six-year study in which two identical model year BEVs were mileage accumulated to 104,000 km, one being charged at AC level 2 (ACL2) and the other being charged at 50kW DC fast-charge (DCFC) [22]. In that study, at approximately the same odometer reading (15,000 km), the UBEs, FRE_{DC}s and FREs of the 2 BEVs had all decreased by approximately 3%, a stark contrast to the results of this study [23]. The higher loss of energy capacity of the newer model year BEVs in this study may be at least partially explained by the effects of calendar fade. Because of the pandemic, the time in between chassis dynamometer rounds 1 and 2 was almost 3 years (33 months), whereas the time span between rounds 1 and 2 for [23] was 6 months. Thus, the combination of 18,000 km mileage accumulation and almost 3 years of calendar fade effects may reasonably be considered the cause of the 8% decrease in UBE for this study's test vehicles.

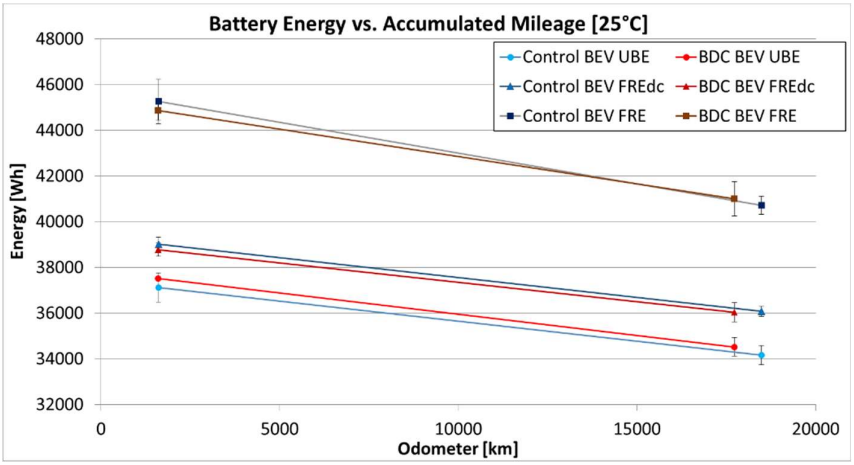

Figure 5: Battery Energies of the Control and BDC BEVs at 1,600 km and 18,000 km odometer

Despite having an additional 220 bi-directional cycles totalling 3.66 MWh of discharge energy, the BDC BEV did not exhibit accelerated FRE, FRE_{DC} or UBE degradation compared to the Control BEV. While tempting to attribute this 3.66 MWh to the number of kilometres that could have been driven using this amount of energy, that comparison is not valid in the context of battery degradation. This is because several factors will influence battery degradation through various mechanisms. Guo et al. (2021) conducted a large overview summary of such mechanisms, which include temperature, depth of discharge (DoD), current (i.e., C-rate), cut-off voltage and State-of-Charge (SoC) as the main factors to consider during charging, driving or standby [2]. All these factors can be vastly different between on-road driving and the V2G testing, and therefore these factors were compared between the different activities in this study.

These C-rates were then binned according to magnitude and the overall number of instances per bin was divided by the total number of measurements made for that file in order to normalize the histograms. Each chassis dynamometer C-rate histogram was averaged by driving cycle, and a sensitivity analysis was performed to determine the effect of testing round, ambient temperature, and vehicle on the spread of the C-rate average for a given drive cycle. This analysis revealed that the Control BEV was driven slightly more aggressively than the V2G vehicle, with approximately 2% more time spent at C-rates > |0.5|.

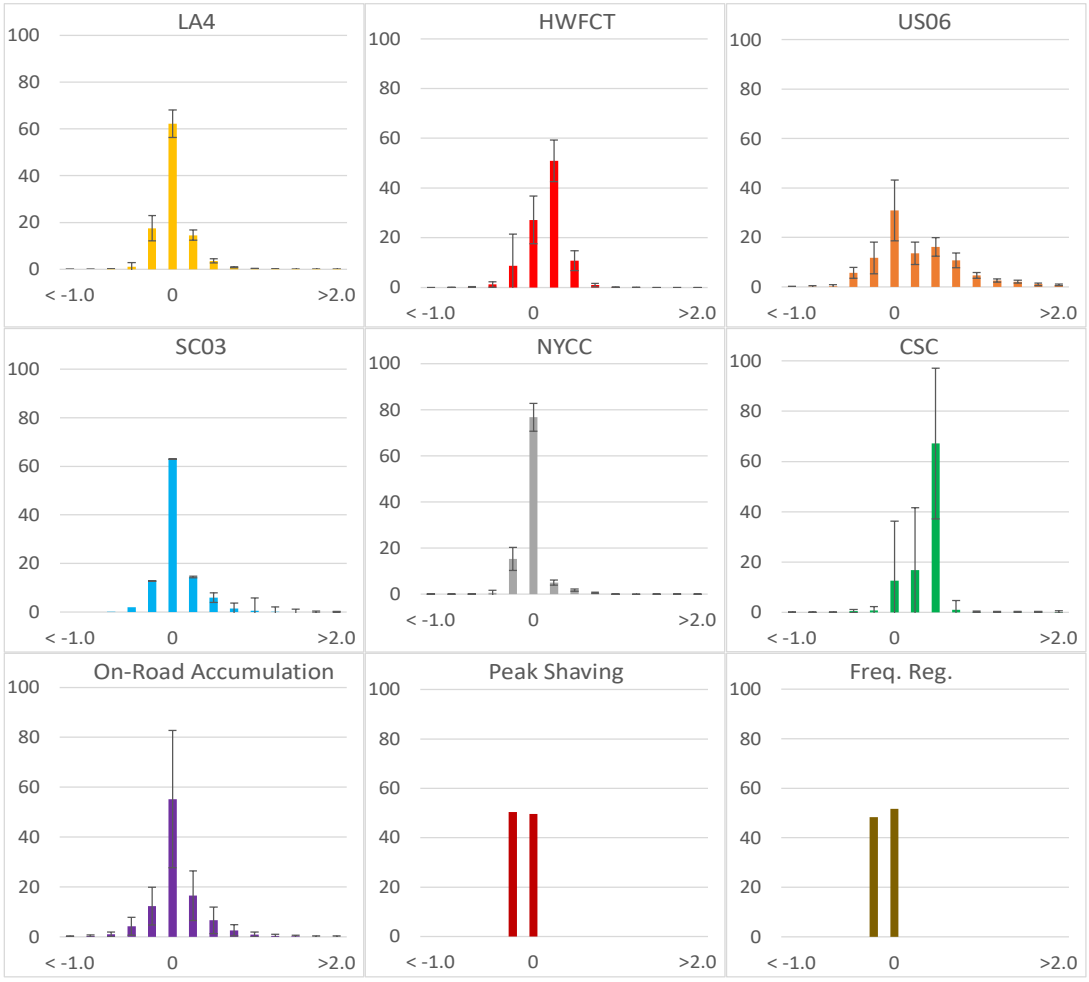

Figure 6: Histograms of battery pack C-rates for both BEVs, averaged for all test rounds and temperatures for each drive cycle, and for all mileage accumulation driving. Peak shaving and frequency shaving histograms are from a single representative day.

Similarly, the mileage accumulation C-rates were averaged for both vehicles together and no significant difference in C-rate profiles was observed between the vehicles. The V2G activity histograms were established using the measured battery currents from one file for peak shaving and one file for frequency regulation because these experiments very tightly controlled the discharge and charge of the vehicles' batteries, and so it was assumed that each file has a very similar current profile.

Figure 6 presents nine average histograms of the battery pack level C-rates exhibited by both vehicles during each type of activity. As can be seen in Figure 6, the SC03 and US06 drive cycles have a right skewed distribution, while the HWFCT and CSC drive cycles have a left skewed distribution, and the mileage accumulation route, and NYCC and LA4 drive cycles have normal distributions; the peak shaving and frequency regulation V2G activities are not distributions, as there is a near 50/50 split between the two lowest C-rate bins. The activities with left-skewed distributions have high, but rather constant loads, while the activities with right-skewed distributions have variable loads owing to highly transient accelerations. The activities with normally distributed C-rate curves are not highly demanding driving traces.

Table 3 presents the amount of time spent outside the ranges of -0.25 and +0.25 C-rates for each activity, as well as the average absolute battery pack current and associated one standard deviation for each activity. In contrast to the highly controlled and low C-rates of the V2G activities, which have zero time outside the range of -0.25C to 0.25C, the drive cycles and the mileage accumulation driving generally spend much more time in the higher magnitude C-rates. Additionally, the drive cycles and mileage accumulation activities

generally have much higher average currents (i.e., C-rates), indicative of the more demanding nature of the loads required for those particular activities.

Table 3: Percent time spent above 0.25C and below -0.25C and average absolute current for each activity

Activity	Time Spent Outside |0.25| C-rate Window	Average Absolute Current and 1 standard deviation [A]
Peak Shaving	0%	19.6 ± N/A
Frequency Regulation	0%	7.3 ± N/A
NYCC	8.0%	8.5 ± 2.1
LA4	20.3%	15.5 ± 2.4
SC03	24.3%	18.8 ± 2.9
Mileage Accumulation	33.2%	25.3 ± 13.3
US06	57.5%	49.6 ± 8.4
HWFCT	61.4%	34.1 ± 6.2
CSC	86.5%	55.14 ± 14.6

It is widely acknowledged that a battery's C-rate will affect the rate of permanent battery degradation [2, 24-27]. This relationship between the C-rate and the battery degradation is impacted to varying degrees by other factors, such as temperature, depth of discharge (DoD), cut-off voltage, charging versus discharging, and state of charge [2]. For instance, Keil et al. (2016) conducted an experimental study on high power lithium-ion cells and determined that high charging currents more strongly shorten cycle life than do high discharge currents [24]. Additionally, Gauthier et al. (2022) conducted experiments on NMC622/NG pouch cells that showed the relationship between battery degradation and C-rate changes for different DoDs [27]. The ambient temperature below which battery degradation is more likely to occur also depends on the C-rate [28]. While some experiments compared relatively high C-rates (i.e., 1C to 5C in Keil P. 2016), other studies have investigated the aging effects of relatively low C-rates (i.e., 1/10C to 1/3C in Gauthier 2022). In either range of C-rates, the relationship is generally the same; a higher discharge C-rate results in more battery degradation over time [24, 27]. In this study, the additional 220 V2G activities on the BDC BEV versus the Control BEV (a total additional energy throughput, charging and discharging combined, of 7.54 MWh) were performed under very precise control that, as Figure 6 and Table 3 point out, completely excluded any activity above a magnitude of 0.25C. The average currents for the peak shaving and frequency regulation activities in Table 3 further emphasize this.

The DoDs of the various activities on the BEVs is shown in Table 4 and taken from the vehicles' CANbus loggers. These DoD numbers were derived for each day of activity and reflect the difference between the highest and lowest SOC, as measured by the CANbus. While FR is conducted in a relatively small SOC window, PS uses a much wider band of SOC, and given both activities were conducted on any particular V2G test day, the median DoD is actually slightly higher than the mileage accumulation activities. And while chassis dynamometer testing used 100% of the vehicles' useable battery capacities, it constituted an overall low percentage of the total activity time for the two BEVs over the duration of this study. Thus, it is unlikely that the vehicles' batteries aged differently in this study due to their DoDs. However, the range within which these activities were performed (i.e. the specific SOC ranges) will greatly impact battery capacity loss.

Table 4: Median Daily Depth of Discharges (DoD) for each activity for the Control and BDC BEVs

Activity	Vehicle	DoD		
		1st Quartile	Median	3rd Quartile
Mileage Accumulation	BDC BEV	20	52	56
	Control BEV	6	49	60
V2G (PS + FR)	BDC BEV	54	56	58
Chassis Dynamometer Testing	Both BEVs	N/A	100	N/A

The SOC, while being directly related to DoD, influences different degradation mechanisms [2]. It has been well established that high resting SOCs will result in accelerated battery degradations [29-32]. In this study, the Control BEV was parked at 100% SOC during the timeframe when the BDC BEV was being V2G tested or set up at the NRC laboratory. This exposure to prolonged periods of high SOC is likely to have contributed to the Control BEV degrading faster than it otherwise would have. Conversely, during BDC activities, the range of useable SOC was limited between approximately 20% and 80%.

While temperature and cut-off voltage are also factors that will influence the impact of different degradation mechanisms in batteries, both vehicles were exposed to the same seasonal temperatures and experienced the

same cut-off voltages. Thus, these two factors would likely not have affected the vehicles differently during this study.

4 Conclusions

Environment and Climate Change Canada, TC and the NRC collaborated to investigate the battery degradation effects of bi-directional charging by mileage accumulating two identical 2018 model year BEVs, and exposing one them to 220 bi-directional cycles, which consisted of highly controlled peak shaving and frequency regulation duty cycles. The vehicles underwent baseline performance testing on chassis dynamometers, and then another round at the conclusion of the bidirectional charging study, in order to quantify any differences in energy capacity, range and energy consumption between them.

The results of this study indicate that after 220 controlled bi-directional charging cycles on the BDC BEV, and approximately 16,000 km of mileage accumulation (between rounds 1 and 2) on both the Control BEV and the BDC BEV, there are neither appreciable nor statistically significant ($\rho = 0.05$) differences in useable battery energy, AC recharge energy and DC received recharge energy degradations between the two vehicles. Bi-directional charging events occurred in the lowest C-rate ranges of all activities and accordingly had the lowest average currents. The vehicles were subjected to similar depth of discharges (DoDs) between the mileage accumulation and bi-directional charging activities, and identical DoDs during chassis dynamometer testing. Both vehicles were also exposed to the same ambient temperatures. However, while the BDC BEV underwent V2G testing, which tightly controlled its SOC between 20% and 80%, the Control BEV was stored at 100% SOC. The combination of the different maximum and range of SOCs, and the very low C-rates of the BDC BEV are suspected to have reduced the observed aging impacts of the additional 7.54 MWh of energy exchange experienced by the BDC BEV to non-statistically significant levels.

This study demonstrates that it is possible to mitigate the battery capacity degradation effects caused by V2G activities by controlling the parameters of bidirectional charging. These results also show how difficult it is to apply a single conversion factor to equate BDC usage to kilometres driven for the purposes of warranties and durability standards. To wit, while 3.66MWh of energy discharge during BDC activities can easily be converted to 16,000 km of driving distance using an energy consumption measurement of 228 Wh/km, 3.66 MWh of BDC usage does not necessarily equate to the battery degradation that would be caused by 16,000 km of driving.

Acknowledgments

The authors would like to acknowledge the essential support to this project provided by the following individuals: Dominique-Pierre Dion for fleet management and mileage accumulation activities, David Buote, Kieran Humphries and Jonah Veenendaal for instrumenting and logging data from the vehicles, Lukasz Sikorski, Maurice Osborne and Paul Dancose for performing the tests at ECCC, and Justin Wilson for assistance with graphics and citations.

References

[1] “Lithium-Ion Batteries Aging Mechanisms”, in *Batteries*, Special Issue, M.F. Sgroi, MDPI, 2021.

[2] J. Guo, Y. Li, K. Pedersen, and D.-I. Stroe, “Lithium-Ion Battery Operation, Degradation, and Aging Mechanism in Electric Vehicles: An Overview,” *Energies*, vol. 14, no. 17, p. 5220, Aug. 2021, doi: 10.3390/en14175220.

[3] Q. Chen and K. A. Folly, “Application of artificial intelligence for EV charging and discharging scheduling and Dynamic Pricing: A Review,” *Energies*, vol. 16, no. 1, p. 146, Dec. 2022., doi: 10.3390/en16010146.

[4] S. Bhoir, P. Caliandro, and C. Brivio, “Impact of V2G service provision on battery life,” *Journal of Energy Storage*, vol. 44, Part A, p. 103178, Dec. 2021, doi: 10.1016/j.est.2021.103178.

[5] M. Jafari, A. Gauchia, S. Zhao, K. Zhang and L. Gauchia, "Electric Vehicle Battery Cycle Aging Evaluation in Real-World Daily Driving and Vehicle-to-Grid Services," in *IEEE Transactions on Transportation Electrification*, vol. 4, no. 1, pp. 122-134, March 2018, doi: 10.1109/TTE.2017.2764320.

[6] C. Guenther, B. Schott, W. Hennings, P. Waldowski, and M. A. Danzer, “Model-based investigation of electric vehicle battery aging by means of vehicle-to-grid scenario simulations,” *Journal of Power Sources*, vol. 239, pp. 604–610, Oct. 2013, doi: 10.1016/j.jpowsour.2013.02.041.

[7] M. Swierczynski, D. -I. Stroe, A. -I. Stan, R. Teodorescu and S. K. Kær, "Lifetime Estimation of the Nanophosphate $LiFePO_4$/C Battery Chemistry Used in Fully Electric Vehicles," *in IEEE Transactions on Industry Applications*, vol. 51, no. 4, pp. 3453-3461, July-Aug. 2015, doi: 10.1109/TIA.2015.2405500.

[8] D. Wang, J. Coignard, T. Zeng, C. Zhang, and S. Saxena, “Quantifying electric vehicle battery degradation from driving vs. vehicle-to-grid services,” *Journal of Power Sources*, vol. 332, pp. 193–203, Nov. 2016, doi: 10.1016/j.jpowsour.2016.09.116.

[9] A. Thingvad, M. Marinelli, “Influence of V2G Frequency Services and Driving on Electric Vehicles Battery Degradation in the Nordic Countries”, presented at EVS31 & EVTeC 2018, Kobe, Japan, Sept. 30 – Oct. 3, 2018, 20189132.

[10] L. Calearo and M. Marinelli, “Profitability of Frequency Regulation by Electric Vehicles in Denmark and Japan Considering Battery Degradation Costs,” *World Electric Vehicle Journal*, vol. 11, no. 3, p. 48, July 2020, doi: 10.3390/wevj11030048.

[11] S. B. Peterson, J. Apt, and J. F. Whitacre, “Lithium-ion Battery Cell Degradation Resulting from Realistic Vehicle and Vehicle-to-Grid Utilization,” *Journal of Power Sources*, vol. 195, no. 8, pp. 2385–2392, April 2010, doi: 10.1016/j.jpowsour.2009.10.010.

[12] K. Uddin, M. Dubarry, and M. B. Glick, “The Viability of Vehicle-to-Grid Operations from a Battery Technology and Policy Perspective,” *Energy Policy*, vol. 113, pp. 342–347, Feb. 2018, doi: 10.1016/j.enpol.2017.11.015.

[13] J. Guo, J. Yang, Z. Lin, C. Serrano and A. M. Cortes, "Impact Analysis of V2G Services on EV Battery Degradation -A Review," *2019 IEEE Milan PowerTech*, Milan, Italy, 2019, pp. 1-6, doi: 10.1109/PTC.2019.8810982.

[14] M. Dubarry, A. Devie, and K. McKenzie, “Durability and Reliability of Electric Vehicle Batteries Under Electric Utility Grid Operations: Bidirectional Charging Impact Analysis,” *Journal of Power Sources*, vol. 358, pp. 39–49, Aug. 2017, doi: 10.1016/j.jpowsour.2017.05.015.

[15] M. Petit, E. Prada, and V. Sauvant-Moynot, “Development of an Empirical Aging Model for Li-ion Batteries and Application to Assess the Impact of Vehicle-to-Grid Strategies on Battery Lifetime,” *Applied Energy*, vol. 172, pp. 398–407, June 2016, doi: 10.1016/j.apenergy.2016.03.119.

[16] Y. Yoo, Y. Al-Shawesh, and A. Tchagang, “Coordinated Control Strategy and Validation of Vehicle-to-Grid for Frequency Control,” *Energies*, vol. 14, no. 9, p. 2530, Apr. 2021, doi: 10.3390/en14092530.

[17] S.R. Ferreira, D.A. Schoenwald, “Duty-Cycle Signal for Frequency Regulation Applications of ESSs”. SAND2013-7315P, Sandia National Laboratories, Albuquerque, New Mexico. 12-Apr-2023 [Online]. Available: http://www.sandia.gov/ess/publications/SAND2013-7315P.xlsx

[18] Government of Canada, “Past Weather and Climate”, 31-Jan-2023. [Online]. Available: https://climate.weather.gc.ca/historical_data/search_historic_data_e.html

[19] Surface Vehicle Recommended Practice, Battery electric vehicle energy consumption and range test procedure, SAE Standard J1634, Rev. April 2021.

[20] Road Load Measurement and Dynamometer Simulation Using Coastdown Techniques, SAE Standard J1263, Rev. March 2010.

[21] U.S. Code of Federal Regulations, EPA dynamometer driving schedules, 40 CFR § 86.115-78 (2023).

[22] A. Loiselle-Lapointe, S. Pedroso, E. Paffumi, M. Safoutin and M. de Gennaro, “Impacts of Mileage Accumulation and Fast Charging on EV Range and Energy Use,” presented at EVS35, Oslo, Norway, June 11-15, 2022, 1780097.

[23] A. Loiselle-Lapointe, I. Whittal and M. Christenson, “Electric Vehicles : Impacts of Mileage Accumulation and Fast Charging,” *World Electric Vehicle Journal*, vol. 8, no. 1, pp. 249-262, March 2016, doi: 10.3390/wevj8010249

[24] P. Keil, A. Jossen, “Charging Protocols for Lithium-ion Batteries and their Impact on Cycle Life-An Experimental Study with Different 18650 High-Power Cells,” *Journal of Energy Storage*, vol 6, pp. 125–141, May 2016, doi: 10.1016/j.est.2016.02.005.

[25] F.B. Spingler, W. Wittmann, J. Sturm, B. Rieger, and A. Jossen, “Optimum Fast Charging of Lithium-ion Pouch Cells Based on Local Volume Expansion Criteria,” *Journal of Power sources*, vol. 393, pp. 152–160, July, 2018, doi: 0.1016/j.jpowsour.2018.04.095.

[26] L. Somerville, J. Bareño, S. Trask, P. Jennings, A. McGordon, C. Lyness and I. Bloom, “The Effect of Charging Rate on the Graphite Electrode of Commercial Lithium-ion Cells: A Post-Mortem Study,” *Journal of Power Sources*, vol. 335, pp. 189-196, Dec. 2016, doi: 10.1016/j.jpowsour.2016.10.002.

[27] R. Gauthier, A. Luscombe, T. Bond, M. Bauer, M. Johnson, J. Harlow, A. J. Louli, and J. R. Dahn, “How do Depth of Discharge, C-rate and Calendar Age Affect Capacity Retention, Impedance Growth, the Electrodes, and the Electrolyte in Li-Ion Cells?,” *Journal of The Electrochemical Society*, vol. 169, no. 2, Feb. 2022, doi: 10.1149/1945-7111/ac4b82.

[28] A. Tomaszewska, Z. Chu, X. Feng, S. O'Kane, X. Liu, J. Chen, C. Ji, E. Endler, R. Li, L. Liu, Y. Li, S. Zheng, S. Vetterlein, M. Gao, J. Du, M. Parkes, M. Ouyang, M. Marinescu, G. Offer and B. Wu, “Lithium-Ion Battery Fast Charging: A Review,” *eTransportation*, vol. 1, 100011, Aug. 2019, doi: 10.1016/j.etran.2019.100011.

[29] J. S. Edge, S. O’Kane, R. Prosser, N. D. Kirkaldy, A. N. Patel, A. Hales, A. Ghosh, W. Ai, J. Chen, J. Yang, S. Li, M.-C. Pang, L. Bravo Diaz, A. Tomaszewska, M. W. Marzook, K. N. Radhakrishnan, H. Wang, Y. Patel, B. Wu, and G. J. Offer, “Lithium ion battery degradation: What you need to know,” *Physical Chemistry Chemical Physics*, vol. 23, no. 14, pp. 8200–8221, March 2021, doi: 10.1039/D1CP00359C.

[30] Z. Gao, H. Xie, X. Yang, W. Niu, S. Li, and S. Chen, “The Dilemma of C-Rate and Cycle Life for Lithium-Ion Batteries under Low Temperature Fast Charging,” *Batteries*, vol. 8, no. 11, p. 234, Nov. 2022, doi: 10.3390/batteries8110234.

[31] A. Millner, "Modeling Lithium Ion Battery Degradation in Electric Vehicles," *2010 IEEE Conference on Innovative Technologies for an Efficient and Reliable Electricity Supply*, Waltham, MA, USA, 2010, pp. 349-356, doi: 10.1109/CITRES.2010.5619782.

[32] T. Waldmann, M. Kasper, and M. Wohlfahrt-Mehrens, “Optimization of Charging Strategy by Prevention of Lithium Deposition on Anodes in High-Energy Lithium-Ion Batteries – Electrochemical Experiments,” *Electrochimical Acta*, vol. 178, pp. 525–532, Oct. 2015, doi: 10.1016/j.electacta.2015.08.056.

Presenter Biography

Aaron Loiselle-Lapointe has more than 11 years of experience testing electric mobility technologies, both on the road and on chassis dynamometers. Previous to this, Aaron conducted in-use emission and fuel consumption tests on marine and locomotive engines. Aaron has a Masters of Applied Science degree in Environmental Engineering and a Bachelor’s of Engineering degree in Aerospace Engineering.